Bioactive Nano-fibrous Scaffold for Vascularized Craniofacial Bone Regeneration

Rahul Damodaran Prabha [a, c, d], David Christian Evar Kraft [d], Linda Harkness [a], Birte Melsen [d], Harikrishna Varma [b], Prabha D Nair [b], Jorgen Kjems [c], Mousthapha Kassem [a*]

[a] Endocrine Research laboratory (KMEB), Department of Endocrinology, University Hospital of Odense,Odense C, 5000, Denmark.

[b]Sree Chitra Tirunal Institute for Medical Sciences and Technology (SCTIMST), Kerala, 695012, India

[c] Interdisciplinary Nanoscience Center (iNANO), Aarhus University, Aarhus C, 8000, Denmark

[d]Section of Orthodontics, Department of Dentistry, Aarhus University, Aarhus C, 8000, Denmark

*Corresponding Author: Rahul Damodaran Prabha , MDS, PhD, Laboratory of Molecular Endocrinology (KMEB), Department of Endocrinology, University of Southern Denmark ,University Hospital of Odense, Winslowparken 25, 1st Floor, DK-5000 Odense C, Denmark. Telephone: +45–65504084; Fax: +45–65919653; E-mail: rahuldp6@gmail.com

This article has been accepted for publication and undergone full peer review but has not been through the copyediting, typesetting, pagination and proofreading process which may lead to differences between this version and the Version of Record. Please cite this article as doi: 10.1002/term.2579

ABSTRACT

There has been a growing demand for bone grafts for correction of bone defects in complicated fractures or tumors in the craniofacial region. Soft flexible membrane like material that could be inserted into defect by less invasive approaches; promote osteoconductivity and act as a barrier to soft tissue in growth while promoting bone formation is an attractive option for this region. Electrospinning has recently emerged as one of the most promising techniques for fabrication of extracellular matrix (ECM) like nano-fibrous scaffolds that can serve as a template for bone formation. To overcome the limitation of cell penetration of electrospun scaffolds and improve on its osteoconductive nature, in this study, we fabricated a novel electrospun composite scaffold of polyvinyl alcohol (PVA) - poly (ε) caprolactone (PCL) - Bioceramic (HAB), namely, PVA-PCL-HAB. The scaffold prepared by dual electrospinning of PVA and PCL with HAB overcomes reduced cell attachment associated with hydrophobic poly (ε) caprolactone (PCL) by combination with a hydrophilic polyvinyl alcohol (PVA) and the bioceramic (HAB) can contribute to enhance osteo-conductivity. We characterized the physicochemical and biocompatibility properties of the new scaffold material. Our results indicate PVA-PCL-HAB scaffolds support attachment and growth of stromal stem cells; (human bone marrow skeletal (mesenchymal) stem cells (hMSC) and dental pulp stem cells (DPSC)). In addition, the scaffold supported *in vitro* osteogenic differentiation and *in vivo* vascularized bone formation. Thus, PVA-PCL-HAB scaffold is a suitable potential material for therapeutic bone regeneration in dentistry and orthopaedics.

Keywords: Bone; Stem cells, Scaffold, Bioceramics; Electrospinning, Craniofacial

1. Introduction

Over the past few decades, there has been a growing demand for bone grafting for correcting bone defects in complicated fractures, following tumor resection or during repair of developmental disorders-associated pathologies in the craniofacial region (Giannoudis, Dinopoulos et al. 2005). Traditionally, autologous bone tissue has been the gold standard for bone grafting. However, donor site morbidity, inadequate supply ,and other associated impedements has encouraged search for alternative sources of bone (Giannoudis, Dinopoulos et al. 2005). A promising alternative source is tissue-engineered bone derived from interaction of stromal skeletal (mesenchymal) stem cells (MSCs),biomaterial scaffolds and growth factors (Mikos, Herring et al. 2006). To be clinically useful, the properties of tissue-engineered bone should “mimic” the native bone tissue (Mikos, Herring et al. 2006).

A large number of scaffolds with a wide number of applications ranging from mere bone filler to more specialized scaffolds have been developed for bone tissue engineering (Kouroupis, Baboolal et al. 2013, Wu, Zhou et al. 2013, Yang, Wang et al. 2013). The scaffolds should provide a supporting surface for MSCs and in addition they are expected to be biocompatible and bioactive (osteoconductive, allowing bone cells to grow on or osteoinductive, inducing new bone formation) as well as biodegradable at the rate of new bone formation(Jones 2013). The scaffolds are also expected to exhibit these ideal properties consistently when fabricated on a large scale, following sterilization and when used clinically(Jones 2013). The craniofacial region contains bones of varying shape, density and morphology and accommodates many vital organs and tissues. The healing of critical bone defects is better with patent vascular supply (Garcia and Garcia 2015) and inhibited by adjacent soft tissue.

Scaffolds which are soft flexible membrane like material that could be inserted into defect by less invasive approaches, promote osteoconductivity and act as a barrier to soft tissue in growth while promoting bone formation is an attractive option for this region. Electrospinning has recently emerged as one of the most promising techniques for fabrication of soft and extracellular matrix (ECM) like nano-fibrous scaffolds that can serve as a template for bone formation. Numerous polymers and natural tissue derivatives have been employed to fabricate scaffolds suitable for use in bone tissues. Poly (**ε**-caprolactone) (PCL) is widely chosen for its biocompatibility and mechanical properties (Ciapetti, Ambrosio et al. 2003). However, PCL exhibit hydrophobicity, which leads to limited cell attachment and also delayed biodegradation (Mohan and Nair 2008).Hydrophobicity of PCL tends to prevent cell migration and prolongs scaffold integration with host tissue(Zhu, Gao et al. 2002). One promising method of reducing hydrophobicity and increasing porosity of PCL is dual electrospinning of PCL with a hydrophilic and biocompatible polymer e.g. poly vinyl alcohol (PVA). PVA also introduces several free hydroxyl chains, which can be employed for scaffold functionalization via linking drugs, biomolecules, or growth factors(Orienti, Bigucci et al. 2001). The electrospun composite of PVA and PCL is food and drug administration (FDA)-approved biomaterial for clinical use. The electrospun PVA-PCL material may be combined with a bioactive bioceramic for improving on osteoconductivity.

HAB is triphasic bioceramic developed by incorporation of hydroxyapatite, beta tricalcium phosphate, calcium silicates and traces of magnesium in a unique combination to act synergistically to produce an osteoconductive and osteoinductive material(Jones 2013) . Magnesium was incorporated to aid in improve sintering window as well as to generate osteo-immunomodulatory effect (Chen, Mao et al.

2014).Incorporation of silicates facilitates bioactivity of scaffold and subsequent vascularization of the scaffold construct (Gorustovich, Roether et al. 2010). It is plausible that PVA and PCL along with an osteoconductive material such as bioactive hydroxyapatite-based triphasic bioceramic (HAB), is an ideal material suitable for craniofacial bone tissue engineering.

To investigate the application of the scaffold for bone regeneration, we tested with the stromal cells, namely, hMSC and DPSC *in vitro*. The hMSC are bone marrow derived skeletal stem cells and widely reported to differentiate into osteoblast upon induction. We also tested DPSC, cells of craniofacial region; to understand possible interaction of cells of neural crest origin on the scaffold. Both the cells served as biological replicates to test wider application of scaffold for bone regeneration in the skeletal system

The present study hence aims to fabricate a novel electrospun composite scaffold PVA-PCL-HAB, with nanofibrous structure and osteoconductive nature, and to investigate its potential role in bone regeneration by combining with bone marrow-derived MSCs or DPSC through *in vitro* and *in vivo* studies in mice models

2. Materials and Methods

2.1 *Scaffold Fabrication and Physicochemical characterization*

2.1.1 *Bioceramic (HAB) Fabrication*

HAB was prepared by refluxing a solution of Tetraethyl-orthosilicate(TEOS) (Sigma-Aldrich, Germany) in ethanol (Sigma Gmbh, Germany). Calcium Nitrate (Rankem, India), Calcium Fluoride (SD Fine, India) and, Magnesium Nitrate (SD Fine, India) dissolved in Orthophosphoric Acid (SD Fine, India) was added to the refluxed TEOS

solution with heating. The mixture was heated and allowed to undergo gelation. The gel formed was dried and calcinated in a Raising-Hearth electric furnace (Bysakh &Co, India) at 600°C for three hrs. The product was then compacted and sintered at 1200 °C for two hr. The obtained product was then milled in a planetary ball mill (Retsch, Germany) at 250 rpm for 20 min. The HAB powder, where then sieved through 20µm sieve (Retsch, Germany).

2.1.2 *Electrospinning*

Ten percent w/v PCL solution (70,000-90,000 Mw, Sigma-Aldrich, USA) was prepared in a mixture of chloroform and methanol (70:30). Ten percent w/v Poly vinyl alcohol (PVA) (89,000-98,000 Mw, Sigma Aldrich, USA) solution was prepared by addition of PVA into boiling distilled water. The 0.5% w/v bioceramic granules were then dispersed in PCL solution by sonication. The electrospinning of scaffolds were performed in a commercially available unit (Holmarc Nanofiber spinning station, India).The dual electrospinning technique employed was with a dual pump and dual syringe system. The spinning parameters are described in (**Table S1**). The electrospun PVA-PCL-HAB obtained were then cross-linked by glutaraldehyde (Sigma Aldrich, USA) solution prepared in 70% Isopropyl alcohol (IP) (SD-Fine chemical limited, India) with Conc. Hydrochloric acid (SD-Fine chemical limited, India) added to the cross-linking solution as a catalyst. The cross linked product was washed in 50% isopropanol and further in water to remove unreacted components. The PVA-PCL-HAB scaffold obtained was then air dried in a laminar flow hood. The morphology of scaffold was imaged with scanning electron microscopy (SEM) (Nova NanoSEM 600; FEI Company, Netherlands and Hitachi S 2400, Japan).

2.1.3 *Physicochemical Characterization*

The chemical compositions of the scaffolds were ascertained by comparing the Fourier Transform Infrared with Attenuated Total Reflectance (FTIR-ATR) spectra of scaffold and its individual components. FTIR-ATR spectra was obtained using ThermoNicolet 5700 FTIR with diamond ATR accessory, in the frequency range of (4000 – 400 cm^{-1}). The thermal stability of the samples was determined by Thermogravimetric Analysis as according to ASTM E1131-03 using Thermogravimetric Analysis-Differential Thermal Analysis (TGA-DTA) instrument (Model SDT 2920 TA Instruments Inc., New Castle, DE).

Water contact angle testing and swelling studies was performed to quantify the hydro-affinity of the scaffolds. The sessile drop method was employed to record water-in-air contact angles of the scaffolds at room temperature (25°C) using a video-based contact angle measuring device (Data Physics OCA15 plus) and imaging software (SCA 20 software) our published protocol (Thomas and Nair 2011).

For the swelling studies, electrospun PVA, electrospun PCL and PVA-PCL-HAB were cut into squares of 100 mm^2 sizes, weighed and immersed in distilled water (pH 7.4) for continuous intervals of time. The strips were removed and carefully blotted using filter paper to remove excess fluid and weighed. The Swelling index calculated by the formula = ((Final weight - Initial weight) / (Initial weight)) ×100

2.1.4 *Ion washout*

PVA-PCL-HAB was cut into 1cm^2 area were immersed in 1mL of phosphate buffered saline (PBS) at 37 °C with pH of 7.4. Total volumes of the PBS were replaced with fresh PBS at day 1, 3, 5, 7 and 14 (Andersen, Offermanns et al. 2013). Ionic

concentration of calcium ions and silica ions released into the washout PBS was quantified with Inductive coupled plasma optical emission spectroscopy (ICP-OES) (5300DV, Perkin Elmer, USA).

2.1.5 *Stimulated Body Fluid (SBF) immersion*

SBF immersion experiment was performed to test the *in vitro* apatite forming ability of the scaffold (Kokubo and Takadama 2006).The scaffolds of 7 mm^2 area were immersed in 10 ml SBF (pH 7.4) and incubated at 37°C for 30 days. The samples collected at days 14 and 30, were washed with deionized water and dried at 37 °C. The apatite formation on the PVA-PCL-HAB were imaged by SEM and analyzed by Energy dispersive X-ray Spectroscopy (EDAX).

2.2 *Cell Culture*

2.2.1 *Cell isolation and characterization*

The DPSC were obtained from therapeutically extracted fully developed impacted healthy third molars from healthy young adult donors. The procedure was performed in accordance with the approved guidelines of The Central Denmark Region Committee on Biomedical Research Ethics. The isolation of DPSC, preparation of culture medium (CM) and osteogenic induction medium (OB) were performed as previously described (Kraft, Bindslev et al. 2010). For bone marrow MSCs, we used the human telomerase immortalized bone marrow derived skeletal stem cell line: hMSC-TERT that has been created in our laboratory and expresses all markers characteristics of primary hMSC including *in vivo* bone formation (Simonsen, Rosada et al. 2002, Al-Nbaheen, Vishnubalaji et al. 2013). For simplicity, we will refer to these cells hereafter as hMSC. All experiments included have a control group

supplemented with CM and an osteogenic differentiation group supplemented with OB.

2.2.2 *MSCs characterization*

Flow cytometry was performed on the cells to evaluate the MSC surface marker expression. DPSC and hMSC, were separately trypsinised to a single cell suspension, were blocked in 2% BSA before incubation with pre-conjugated antibodies, or matched isotype controls (**Table S3**), for 45 min on ice. All samples were washed in FACS buffer (PBS, 40 nM EDTA and FBS 2%) and were analyzed with Beckman Coulter Cell Lab Quanta^{TM} SC and WinMdi software.

2.2.3 *Cell Seeding, Attachment, Spreading and Proliferation*

The PVA-PCL-HAB scaffolds of 3mm diameter were punched out using biopsy punch (Kai Europe GmbH, Germany). Scaffolds were sterilized in 70 % ethanol for thirty min, followed by washing thrice in sterile water and further sterilized by dried under UV light (Rainer, Centola et al. 2010) for 30 min. Prior to seeding, the scaffolds were conditioned by wetting with culture media to obtain uniform seeding. The conditioned scaffolds placed in ultra-low adhesion tissue culture plates (Costar, Corning) were seeded with 3×10^4 cells in 5 µl per scaffold. Scaffolds were then incubated at 37 °C, 5% CO_2 for 45 min to allow cell attachment. The CM was supplemented immediately after the cell attachment. Osteogenic induction was initiated at 24 hrs , post seeding.

Cell attachment and proliferation on the PVA-PCL-HAB were assessed by DAPI/Phallodin staining and Cell Titre- Blue (Promega, Madison, USA) assay respectively for time points 1, 2, 5 and 7 days. DAPI/ Phalloidin staining were

performed as per, protocol (Andersen, Offermanns et al. 2013).The stained PVA-PCL-HAB were imaged under Olympus FV1000MPE Confocal microscope for DAPI (359 nm) and Phallodin (550 nm) respectively.

Cell spreading on scaffolds were examined by SEM. PVA-PCL-HAB seeded with lower cell density 1000 cells/ scaffolds were fixed in 2.5% glutraldehyde for one hour, washed in PBS and dehydrated in graded series of alcohol and SEM performed at conditions stated previously (Shabani, Haddadi-Asl et al. 2014). The spreading of cells on scaffolds was imaged at 1, 5, 10 and 15 days. The proliferation of cells seeded on the scaffolds was estimated by number of viable cells Using Cell Titer-Blue reagent (Promega, Madison, USA). The absorbance measured was normalized to the standard linear curve established to obtain cell number. The assumption made was cells are not metabolically active until 24 hr.

2.2.4 *ALP activity*

Alkaline phosphatase (ALP) activity was measured by using enzymatic *p*-nitrophenyl phosphate (Sigma-Aldrich) substrate reduction and further, normalized against the cell number. Cell number was quantified by the addition of Cell Titer-Blue reagent to culture medium, incubating at 37 °C for 1 hr., and measuring fluorescent intensity ($560_{EX}/590_{EM}$). Samples were then washed with PBS and Tris-buffered saline, fixed with 3.7% formaldehyde in 90% ethanol for 30 s at room temperature, incubated with substrate (1 mg/ml of *p*-nitro phenyl phosphate in 50 mM $NaHCO_3$, pH 9.6, and 1 mM $MgCl_2$) at 37 °C for 20 min, and the absorbance measured at 405 nm (Qiu, Hu et al. 2010).ALP activity was normalized to cell number. ALP activity of cells on tissue culture plates (Plastic) with CM and OB were used as positive controls.

2.2.5 *Cytochemical staining*

ALP staining (Harkness, Mahmood et al. 2011) and Alizarin red staining (AZR) (Harkness, Mahmood et al. 2011) (Sigma-Aldrich, Denmark) for osteogenic differentiation was performed post-fixation using either ice cold 70% ethanol for 1 hr. (AZR) or 0.10 mM citrate buffer pH 4.2/acetone fix (ratio 3:2) for 5 min at room temperature (ALP). ALP staining was carried out with a (ratio 1:1)solution mix of 0.2 mg/ml Napthol AS-TR phosphate substrate (Sigma-Aldrich, Denmark) in water and 0.417 mg/ml of Fast red (Sigma-Aldrich, Denmark) in 0.1 M Tris (pH 9.5) for 1 hr. at room temperature. Samples for AZR staining were incubated in 40 mM AZR at pH 4.2 for 10 min at room temperature followed by washing in distilled water and PBS, before examination for the presence of mineralized matrix.

2.2.6 *Osteogenic Gene expression*

Cell seeded on PVA-PCL-HAB and the controls, cells seeded on culture plates (Plastic) were lysed for total RNA extraction using Trizol (Invitrogen, Denmark); according to manufacturer's instructions The RNA pellets obtained were quantified using NanoDrop1000 spectrophotometer v3.7 instrument (Thermo Fisher Scientific, U.S.A). cDNA were constructed using a revertAid H minus first strand cDNA synthesis kit (Fermentas, St Leon-Rot, Germany) according to the manufacturer's instructions. RT-qPCR analysis was performed with StepOnePlus^{TM}system (Applied Biosystems, Denmark)..Following normalization to reference genes, quantification of relative gene expression was carried out using a comparative CT method at day 15. The expression of osteogenic markers RUNX2, alkaline phosphatase (ALP), Collagen 1α1 (COL1a1), Osteocalcin (BGLAP), Osteonectin (SPARC), and Osteopontin (SPP1) were compared with controls. The sequence of Primers (Eurofin

MSW Operon, UK) used for RT-qPCR reaction are depicted in supplementary information (**Table S4**).

2.3. *Ectopic bone formation*

All *in vivo* experiments were performed under the permission from Danish National Ethical committee on animal experiments. Danish regulations for care and use of laboratory animals were maintained throughout the experiments. Ectopic bone formations on cell seeded scaffolds were tested by implantation of cell laden scaffolds subcutaneously in NOD.CB17-*Prkdc*^{scid}/J mice as per our lab protocol (Abdallah, Ditzel et al. 2008). 5×10^5 cells were seeded on scaffolds *in vitro* and were implanted subcutaneously. Each mouse had four implants, two were the cell laden PVA-PCL-HABs and other two implants were cells seeded on 40mg hydroxyapatite-tricalcium phosphate (HA/TCP, Triosite 0.5 – 1mm granules, Biomatlante/Zimmer, Vigneux de Bretagne, France), which served as the control (Harkness, Mahmood et al. 2011). DPSC (n = 4) and hMSC (n = 4), seeded scaffolds were used in separate mice. Eight weeks after implantation, the scaffolds and implants was removed and fixed in 4% Paraformaldehyde and decalcified with 0.38 M EDTA before embedding in paraffin. Sections were stained with Haematoxylin and Eosin (H&E), human Vimentin antibody(VM) (clone SP20,Thermo Scientific) and Collagen Type I antibody (Col Type I) (LF-67 kindly provided by Dr. Larry Fisher, the National Institute of Dental and Craniofacial Research, National Institutes of Health) and Sirius red in picric acid(Sirius red F3BA), imaged under polarized light.

2.3.3 *Statistical Analysis*

All *in vitro* experiments were performed in at least in triplicates. The data represented are mean ± standard error of the mean. The comparisons between groups were

carried out by analysis of variance (ANOVA) with multiple comparisons followed by Tukey post hoc test. *t* - Tests were performed when only two groups were compared. Statistical analysis was performed using GraphPad Prism (version 6.00, GraphPad Software, La Jolla California USA). *P* values < 0.05 were considered significant.

3. RESULTS

Physiochemical Characterization of PVA-PCL-HAB scaffold

The PVA-PCL-HAB was fabricated using the electrospinning process with dual pump and dual syringe. (**Fig. 1A),** shows fiber morphology visualized by SEM. The fibers are smooth, randomly aligned and formed a sheet consisting of interpenetrating network of thick (1000±240 nm; n = 60) and thin fibers (230±100 nm; n = 60).The pores in range from 2µm - 20 µm, were measured from SEM images. The bioceramic HAB particles dispersed in PCL solution during scaffold manufacturing adhere to the thick fibers with visible granules (**Fig. 1A**).

The IR spectra (**Fig.1B**) exhibited characteristic peaks of individual polymers PVA and PCL as well as pure HAB and PVA-PCL-HAB. The spectra of pure polymer PCL show characteristic IR bands (**Table S2**)of 1721 cm^{-1} attributed to C=O stretching (str), and C-O str bands at 1238 cm^{-1} and 1292 cm^{-1}. C-O-C str frequencies of 1164 cm^{-1} ,1108 cm^{-1} and 1049 cm^{-1} and the 2941 $cm^{-1}$are attributed to the asymmetric (Asy.str) of CH_2 bands. All the typical bands for PCL were also seen in PVA-PCL-HAB. Characteristic broad peaks at 3259 cm^{-1}attributed to OH str and CH_2 vibration (Vib) band at 1417 cm^{-1} were seen in both pure PVA and PVA-PCL-HAB. Characteristic 1050 cm^{-1}peak attributed to Si-O-Si strand 960,934, 583, and 546 cm^{-1}peaks, attributed to PO_4^{3-}ions were observable in pure HAB and PVA-PCL-HAB.

These data confirms that all polymers and bioceramic particles are present in the material.

Thermal stability was assessed by Thermo gravimetric analysis (TGA) studies. TGA thermogram of electrospun PVA, PCL, and the PVA-PCL-HAB scaffolds shows that the materials are thermally stable at 37 °C (**Fig.1E**) and the thermogram of PVA showed the onset of decomposition at about 60 °C caused by the loss of water present in the scaffold. The second decomposition demonstrates breaking up of C-H bonds. The temperature at which 50% of the mass loss occurs is generally considered as a measure of thermal stability. In the case of PVA, 50% mass is remaining at 299°C and 7.34% mass is remaining at 494°C. PCL has good thermal stability with onset of decomposition near to 330 °C, and mass loss was less than 8% even at 353 °C. Half of mass is remaining at 395°C and 0.6% mass only is remaining at 494°C. The thermal stability of PCL is significantly greater than that of PVA. The thermal degradation pattern of the hybrid scaffold PVA-PCL-HAB tended to become similar to PCL. The hybrid material thus has a very good thermal stability with 50% mass loss at a slightly elevated temperature of 398°C.

The hydrophilicities of the materials were assessed by studying their water absorption capacity and their air- water contact angles. Water contact angle measurements of PVA scaffolds and PCL scaffolds were (80.27°±11.8) and (124°± 3.7) respectively (**Fig. 1C**). The combination of PVA fibers and PCL fibers showed significant increase in hydrophilic affinity (98.85°± 9.6; $P< 0.05$) of PVA-PCL-HAB, when compared with PCL scaffold. PCL is hydrophobic and its swelling index at pH 7.4 was around 260 %. PVA on the other hand has been reported to be hydrophilic and we observed a higher swelling of around 450%. Co- electrospinning PCL and the hydrophilic PVA increased the hydrophilicity and water absorption capacity of the

hybrid material. As shown in (**Fig. 1D**) the water absorption capacity estimated by swelling of the hybrid material is around 350 % which lies between the values observed for the individual polymers. Thus, the swelling studies ensure that the hydrophilic/ hydrophobic tuning can be achieved by appropriate co-electrospun blends of materials. Incorporation of silica particles has been reported to reduce hydrophobicity of PCL (Lee, Teng et al. 2010). Water contact angle measurements for surface hydro affinity properties showed that the PVA-PCL-HAB scaffold had a mean contact angle significantly reduced compared to electrospun PCL under similar testing conditions. Our results indicated there is no significant change in water contact angle measurement following addition of HAB to PCL. The swelling ratio analysis showed the swelling capacity of PVA-PCL-HAB was at an intermittent percentage of 350% between the higher swelling ratio of PVA and lower swelling ratio of PCL. The higher swelling ratio favors the perfusion of nutrients required for cell growth(Shanmugasundaram, Ravichandran et al. 2001). The increased swelling ratio would also facilitate free ionic exchange from the scaffold

ICP-OES analysis of the washout collected showed significant gradient increase in cumulative ion release of calcium and silica from the PVA-PCL-HAB until a plateau was reached at day7 (**Fig . 1F**). The ion release profile also indicates that PVA-PCL-HAB was able to deliver calcium and silica ions essential for the initiation of bioactive response.

SBF immersion

The apatite depositions on the biomaterial surfaces upon immersion in SBF were reported to be predictive for *in vivo* bone bonding ability. The SEM image of PVA-PCL-HAB samples immersed in SBF for 30 days showed accumulation of apatite like

crystals (**Fig.1 G**) .The EDAX analysis of the crystals confirmed apatite deposition with peaks of calcium and phosphorous (**Fig.1 G**).

Cell Characterization

Both hMSC and DSPC exhibited similar stromal cell-like morphology (**Fig. S1)**. Flow cytometry analysis showed that both hMSC and DPSC express characteristics MSC surface markers: $CD44^+$, $CD73^+$, $CD90^+$, $CD105^+$, and $CD166^+$and $CD14^-$(**Fig.S1**). hMSC cultures contained increased numbers of $CD63^+$ and $CD146^+$cells as compared to DPSC. DPSC had a mixed CD146 positive phenotype

Cell Viability, Proliferation and Spreading

DAPI and Phallodin staining at day one post cell seeding on PVA-PCL-HAB; (**Fig. 2 (I)**) revealed good cell attachment as evidenced by the presence of elongated actin filaments. By day 7, the cells were evenly distributed throughout the scaffold. Both hMSC and DPSC proliferated efficiently on the PVA-PCL-HAB scaffold. Cell number as estimated by cell-Titre blue assay revealed increased cell number up to 7 days post-seeding (**Fig. 2 (II)**). SEM analysis showed both hMSC and DPSC attach, proliferate and spread on the scaffold surface (**Fig.2 (III)**). Both cell types formed confluent cell sheet with only limited visible on PVA-PCL-HAB surface by day 15.

ALP Activity

We employed ALP activity as a marker for osteoblastic lineage commitment. The ALP activities of both cell lines were compared when cultured on plastic surfaces and on PVA-PCL-HAB scaffold. Both cell types increased their ALP activity in response to osteoblast induction media. However, we observed some quantitative differences in ALP activity. For hMSC the maximal ALP activity was observed at day

10 when cultured on plastic and on day 15 when cultured on PVA-PCL-HAB scaffold **(Fig. 3A)** and there was no significant difference in maximal ALP activity. For DPSC, ALP activity was low when cultured on plastics compared to PVA-PCL-HAB scaffold. Similar to hMSC, maximal ALP activity was observed on day 15 when cultured on PVA-PCL-HAB scaffold **(Fig. 3C)**.Similar results were obtained from cytochemical staining for ALP of cultured cells on plastic and on PVA-PCL-HAB scaffold(**Fig.3 B,D**)

Ex vivo mineralization

The ability of PVA-PCL-HAB scaffold to support the formation of in vitro mineralized matrix was examined. Following in vitro osteoblast differentiation induction, cells cultured on plastics and on PVA-PCL-HAB scaffold were examined for the presence of mineralized matrix as visualized by Alizarin red staining. Both cell types formed mineralized matrix at day 15 post osteoblast differentiation, when cultured on plastics **(Fig.3 E**) and similar pattern was observed on PVA-PCL-HAB scaffold. However, hMSC exhibited more intense staining (**Fig.3 E**).

Ex vivo Osteoblastic gene expression

We also examined for the ability of PVA-PCL-HAB scaffold to maintain the differentiated osteoblastic phenotype compared to standard plastic culture surfaces. The expressions of RUNX2, Col1a1, ALP, SPARC, SPP1 and BGLAP, mRNA were quantitated at day 15 following in vitro osteoblast differentiation induction (**Fig.4**). Both hMSC and DPSC expressed osteoblast gene markers when cultured on plastic and on PVA-PCL-HAB scaffold **(Fig.4)**. However, some markers exhibited quantitative differences when the cells were cultured on plastic versus PVA-PCL-HAB scaffold. For hMSC **(Fig. 4 A),** Col1a1 expression was higher when cells

cultured on plastics whereas SPP1 was higher when cells were cultured on PVA-PCL-HAB scaffold. Similarly, DPSC exhibited a dramatic upregulation expression of SPP1 when cultured on plastic compared to cells cultured on PVA-PCL-HAB scaffold **(Fig. 4B).**

In vivo ectopic bone formation

All mice implanted with PVA-PCL-HAB scaffolds were healthy, gained weight and had no signs of inflammation during the experiment. Eight weeks post subcutaneous implantation in immune deficient mice; PVA-PCL-HAB implants were vascularized as seen by visual inspection (Fig. **5** and **inset**). Histologic examination (Fig. **5**) showed areas of bone formation in implants containing either hMSC or DPSCs as evidenced by the presence of a positive stain of type I collagen and the presence of characteristics birefringence of organized collagen type I (Sirius Red F3BA). These matrixes were produced by the cells of human origin, as evidenced by positive staining of human specific anti-VM antibody (**Fig.5**).

4. Discussion

The aim of the present study was to develop a biodegradable and less invasive electrospun biomaterial that supports skeletal stem cell osteoblastic differentiation and bone formation with vascularization in the peripheral and craniofacial skeleton. In the present study, we have demonstrated that an electrospun PVA-PCL-HAB scaffold can support osteoblast differentiation of two types of stem cells relevant to bone tissue regeneration: bone marrow derived skeletal stem cells and dental pulp stem cells as well as in vivo ectopic bone model.

We fabricated an electrospun scaffold with nano fibrous porous structure to mimic the native extracellular matrix of bone (Holzwarth and Ma 2011, Wang, Ding et al. 2013). The PVA-PCL-HAB scaffold comprises a dual electrospun network of PCL and PVA which has incorporated HAB bioceramic to facilitate osteoconductivity. Hydrophilic PVA is included in the scaffold as it degrades faster than PCL and thus reducing the bulk of the scaffold as new bone is formed. The combination of PVA and PCL is used for enhancing the hydrophilicity; cell attachment allows better cell penetration upon attachment. We have also included in the scaffold a bioceramic: HAB. Bioceramics support bone formation by hydroxycarbonate apatite (HCA)(Hench and Paschall 1973). The HAB used for scaffold fabrication was a triphasic bioceramic (an amorphous mixture of hydroxyl apatite (HA), beta tricalcium phosphate (TCP) and calcium silicate and traces of magnesium).The optimized concentration of magnesium was added to improve sintering window without affecting bioactivity (Ma, Chen et al. 2010) . The incorporation of magnesium along with beta tricalcium phosphate has been reported to generate an osteo-immunomodulatory effect and inhibit osteoclastogenesis (Chen, Mao et al. 2014).

We mixed HAB with PCL before electrospinning to produce electrospun PVA-PCL-HAB composite. The anticipated bioactive mechanism is based on HAB releasing calcium and phosphate ions upon contact with body fluids that raise local pH and form a silica rich interface as well as facilitating surface mobilization and accumulation of amorphous apatitic calcium phosphate phase. Assimilation of hydroxyls and carbonates from the solution by the apatitic calcium phosphate phase leads to reorganization and deposition of HCA. The HCA layer binds to the host bone by its interaction with collagen fibrils of the native bone. We employed a number of technologies to confirm the expected biophysical characteristics of PVA-

PCL-HAB scaffold. The SEM images confirmed that the electrospinning of PVA-PCL-HAB resulted in nanofibrous porous network. The presence of bioceramic granules on the thick fibers denote that thick fibers were PCL and the EDAX spectra of the granules also confirmed the elemental peaks of calcium, phosphate, silica and magnesium. The FTIR spectral peaks confirm the presence of PCL, PVA and HAB in the electrospun scaffold. The thermal stability data confirmed the stability of the PVA-PCL-HAB was comparable to highly stable PCL and the thermal stability was also considerably higher than PVA. The PVA-PCL-HAB scaffold depicted the typical characteristic peaks of all the constituent individual materials with no evidence of covalent interactions. Hence, the composite material maintains the characteristics of the constituent materials and act as a synergistic blend (Mohan and Nair 2008).

Ion washout release profile studies demonstrated that calcium and silica ions were released from PVA-PCL-HAB scaffold. The release of calcium and silicion increased until day 7, where it attained a plateau. The lower levels of released silicon ions when compared with calcium ions released were proportional to the lower percentage of silicates incorporated while fabrication of HAB. Silicon ions are only required for initiation of bioactive reaction, while the progression of reaction and completion of the reaction would be governed by calcium and phosphate complex (Hench 1991)

We tested the hypothesized bioactivity and bone bonding of the scaffold by SBF immersion experiments in accordance with the proposal by Kokubo et al, that any bone boding surface is expected to produce apatite like structure upon immersion in SBF for a period of four weeks (Kokubo and Takadama 2006). SEM images of the SBF immersed PVA-PCL-HAB showed surface deposition of apatite like crystals at

day 30. The EDS examination of crystals showed increased calcium and phosphate peaks indicative of apatite crystal formation.

We tested two stromal derived stem cells: DPSC and hMSC. DPSC, are stem cells of neural crest origin (Arthur, Rychkov et al. 2008, La Noce, Mele et al. 2014) whereas hMSC are bone marrow derived skeletal stem cells of mesodermal origin; both the stem cells are capable of bone formation in craniofacial region (Tollemar, Collier et al. , La Noce, Mele et al. 2014, Tollemar, Collier et al. 2016). Generally both cell types exhibited similar phenotype but we observed some quantitative differences. Fewer CD146 expressing cells were present in DPSC cultures compared with bone marrow hMSC. CD146 expressions has been reported to associated with osteogenic potential of bone marrow hMSC(Sacchetti, Funari et al. 2007).

We observed that both hMSC and DPSC attached readily to the PVA-PCL-HAB scaffold and more than 70 % of the seeded cells attached at day 1 post seeding. Cell attachment on the scaffold surface is dependent on the method of seeding and hydro-affinity of the scaffold surface. We employed the sessile drop high density seeding method that has been reported to provide maximal cell attachment (Reynolds, Riehle et al. 2014).

PVA-PCL-HAB scaffold with its balanced hydrophobic-hydrophilic properties supported cell viability and proliferation of both bone marrow hMSC and DPSC. Both cell types were seen to be uniformly distributed, viable and proliferating on the scaffold. However, the three dimensional distribution of the cells in the scaffold 3D architecture impedes its quantification. Hence we adopted the cell titer blue assay to quantify the average number of viable cells present at different time points. The

hMSC were seen to proliferate at significantly higher rate at day 7 when compared to DPSC which continued at stationary phase.

The ability of PVA-PCL-HAB scaffold to support osteoblastic differentiation of hMSC and DPSC cells were tested using a number of criteria: ALP activity, osteoblastic gene expression and the ability to form mineralized matrix. While we observed similar results between hMSC and DPSC, there were quantitative differences in the levels of ALP activity or osteoblastic gene expression, that can be explained by differences in cell confluence and cell number as these factors may exert additional effects independent of the differentiated status of the cells (Tomlinson, Dennis et al. 2015). In addition to the ability of PVA-PCL-HAB scaffold to support *in vitro* osteoblast differentiation of DPSC and hMSC, it supported bone formation *in vivo* in an ectopic bone formation model. We observed good vascularization of the PVA-PCL-HAB scaffold which may be linked to stimulated local production of VEGF by the dissolute products of HAB(Day, Boccaccini et al. 2004). Histological analysis of the implants demonstrates the ability of the PVA-PCL-HAB scaffold to support bone formation. The *in vivo* implantations without inducing the seeded cells also confirm the ability of scaffold to receive molecular cues from host tissue and synchronize bone formation. The material could hence be used as a soft and less invasive scaffold for bone defects of the craniofacial region.

The highlighting feature of the study was to reproduce the *in vitro* bone formation results in an *in vivo* setting even in the absence of osteogenic induction through using appropriate biomaterial of the study. These *in vivo* studies provide a supportive data to the first time report of potential clinical use of this scaffold in contrast to any other previously reported polymer based biomaterials.

5. Conclusions

In this study we have developed an electrospun PVA-PCL-HAB scaffold with a hydrophobic-hydrophilic nature and promoting osteoconductivity. The scaffold has ability to support proliferation, osteoblastic differentiation and bone formation for two different stem cell types; hMSC and *DPSC in vitro*. The biomaterial further supports skeletal stem cell osteoblastic differentiation and bone formation with vascularization *in vivo.* These results encourage testing of this material for therapeutic applications of bone regeneration in the field of orthopedics and dentistry. Hence we recommend PVA-PCL-HAB scaffold with multiple applications as an ideal material for vascularized craniofacial bone tissue engineering. Further studies with craniofacial defects in mice and large animal models are planned in future.

6. Acknowledgements

Authors would like to acknowledge Nicholas Ditzel for help with implantation studies, Lone Christiansen, for technical assistance with histological processing of the implants. We thank Lisbeth A. Abildtrup, Aarhus Dental School for isolation of DPSC, Ulla Melchior Hansen, Danish Molecular Biomedical Imaging Center for assistance in confocal imaging, and Dr. S. Suresh Babu and Dhanesh Vaikkat from SCTIMST, India for assistance in fabrication of scaffold. Authors also thank Nimi N, DTERT, and SCTIMST for technical assistance. The study was supported by an Indo-Danish grant obtained from The strategic research council of Denmark and Department of Biotechnology; India. his work was also supported Lund beck Foundation Nano medicine Center for Individualized Management of Tissue Damage and Regeneration. The funding bodies provided monetary support only.

Authors Contibutions

Concept, designing of experiments, analytical interpretation of results and manuscript preparation: RDP, DCK, BM, HKV, PDN, JK, and MK. Cell characterizations and experiment protocols establishment: RDP & LH. Biomaterial designing and characterization: RDP, HKV and PDN

Disclosures

No potential conflicts of interest exist.

References

Abdallah, B. M., N. Ditzel and M. Kassem (2008). Assessment of Bone Formation Capacity Using In vivo Transplantation Assays: Procedure and Tissue Analysis. Osteoporosis: Methods and Protocols. J. J. Westendorf. Totowa, NJ, Humana Press**:** 89-100.

Al-Nbaheen, M., R. Vishnubalaji, D. Ali, A. Bouslimi, F. Al-Jassir, M. Megges, A. Prigione, J. Adjaye, M. Kassem and A. Aldahmash (2013). "Human stromal (mesenchymal) stem cells from bone marrow, adipose tissue and skin exhibit differences in molecular phenotype and differentiation potential." Stem Cell Rev **9**(1): 32-43.

Andersen, O. Z., V. Offermanns, M. Sillassen, K. P. Almtoft, I. H. Andersen, S. Sorensen, C. S. Jeppesen, D. C. Kraft, J. Bottiger, M. Rasse, F. Kloss and M. Foss (2013). "Accelerated bone ingrowth by local delivery of strontium from surface functionalized titanium implants." Biomaterials **34**(24): 5883-5890.

Arthur, A., G. Rychkov, S. Shi, S. A. Koblar and S. Gronthos (2008). "Adult human dental pulp stem cells differentiate toward functionally active neurons under appropriate environmental cues." Stem Cells **26**(7): 1787-1795.

Chen, Z., X. Mao, L. Tan, T. Friis, C. Wu, R. Crawford and Y. Xiao (2014). "Osteoimmunomodulatory properties of magnesium scaffolds coated with beta-tricalcium phosphate." Biomaterials **35**(30): 8553-8565.

Ciapetti, G., L. Ambrosio, L. Savarino, D. Granchi, E. Cenni, N. Baldini, S. Pagani, S. Guizzardi, F. Causa and A. Giunti (2003). "Osteoblast growth and function in porous poly epsilon -caprolactone matrices for bone repair: a preliminary study." Biomaterials **24**(21): 3815-3824.

Day, R. M., A. R. Boccaccini, S. Shurey, J. A. Roether, A. Forbes, L. L. Hench and S. M. Gabe (2004). "Assessment of polyglycolic acid mesh and bioactive glass for soft-tissue engineering scaffolds." Biomaterials **25**(27): 5857-5866.

Giannoudis, P. V., H. Dinopoulos and E. Tsiridis (2005). "Bone substitutes: An update." Injury **36**(3, Supplement): S20-S27.

Gorustovich, A. A., J. A. Roether and A. R. Boccaccini (2010). "Effect of bioactive glasses on angiogenesis: a review of in vitro and in vivo evidences." Tissue Eng Part B Rev **16**(2): 199-207.

Harkness, L., A. Mahmood, N. Ditzel, B. M. Abdallah, J. V. Nygaard and M. Kassem (2011). "Selective isolation and differentiation of a stromal population of human embryonic stem cells with osteogenic potential." Bone **48**(2): 231-241.

Hench, L. L. (1991). "Bioceramics: From Concept to Clinic." Journal of the American Ceramic Society **74**(7): 1487-1510.

Hench, L. L. and H. A. Paschall (1973). "Direct chemical bond of bioactive glass-ceramic materials to bone and muscle." Journal of Biomedical Materials Research **7**(3): 25-42.

Holzwarth, J. M. and P. X. Ma (2011). "Biomimetic nanofibrous scaffolds for bone tissue engineering." Biomaterials **32**(36): 9622-9629.

Jones, J. R. (2013). "Review of bioactive glass: From Hench to hybrids." Acta Biomater **9**(1): 4457-4486.

Kokubo, T. and H. Takadama (2006). "How useful is SBF in predicting in vivo bone bioactivity?" Biomaterials **27**(15): 2907-2915.

Kouroupis, D., T. G. Baboolal, E. Jones and P. V. Giannoudis (2013). "Native multipotential stromal cell colonization and graft expander potential of a bovine natural bone scaffold." J Orthop Res **31**(12): 1950-1958.

Kraft, D. C., D. A. Bindslev, B. Melsen, B. M. Abdallah, M. Kassem and J. Klein-Nulend (2010). "Mechanosensitivity of dental pulp stem cells is related to their osteogenic maturity." Eur J Oral Sci **118**(1): 29-38.

La Noce, M., L. Mele, V. Tirino, F. Paino, A. De Rosa, P. Naddeo, P. Papagerakis, G. Papaccio and V. Desiderio (2014). "Neural crest stem cell population in craniomaxillofacial development and tissue repair." Eur Cell Mater **28**: 348-357.

Lee, E. J., S. H. Teng, T. S. Jang, P. Wang, S. W. Yook, H. E. Kim and Y. H. Koh (2010). "Nanostructured poly(epsilon-caprolactone)-silica xerogel fibrous membrane for guided bone regeneration." Acta Biomater **6**(9): 3557-3565.

Ma, J., C. Z. Chen, D. G. Wang, Y. Jiao and J. Z. Shi (2010). "Effect of magnesia on the degradability and bioactivity of sol–gel derived SiO2–CaO–MgO–P2O5 system glasses." Colloids and Surfaces B: Biointerfaces **81**(1): 87-95.

Mikos, A. G., S. W. Herring, P. Ochareon, J. Elisseeff, H. H. Lu, R. Kandel, F. J. Schoen, M. Toner, D. Mooney, A. Atala, M. E. Van Dyke, D. Kaplan and G. Vunjak-Novakovic (2006). "Engineering complex tissues." Tissue Eng **12**(12): 3307-3339.

Mohan, N. and P. D. Nair (2008). "Polyvinyl alcohol-poly(caprolactone) semi IPN scaffold with implication for cartilage tissue engineering." J Biomed Mater Res B Appl Biomater **84**(2): 584-594.

Orienti, I., F. Bigucci, G. Gentilomi and V. Zecchi (2001). "Self-assembling poly(vinyl alcohol) derivatives, interactions with drugs and control of release." J Pharm Sci **90**(9): 1435-1444.

Qiu, W., Y. Hu, T. E. Andersen, A. Jafari, N. Li, W. Chen and M. Kassem (2010). "Tumor necrosis factor receptor superfamily member 19 (TNFRSF19) regulates differentiation fate of human mesenchymal (stromal) stem cells through canonical Wnt signaling and C/EBP." J Biol Chem **285**(19): 14438-14449.

Rainer, A., M. Centola, C. Spadaccio, G. Gherardi, J. A. Genovese, S. Licoccia and M. Trombetta (2010). "Comparative study of different techniques for the sterilization of poly-L-lactide electrospun microfibers: effectiveness vs. material degradation." Int J Artif Organs **33**(2): 76-85.

Reynolds, P. M., M. Riehle and N. Gadegaard (2014). Cell seeding method and device, Google Patents.

Sacchetti, B., A. Funari, S. Michienzi, S. Di Cesare, S. Piersanti, I. Saggio, E. Tagliafico, S. Ferrari, P. G. Robey, M. Riminucci and P. Bianco (2007). "Self-Renewing Osteoprogenitors in Bone Marrow Sinusoids Can Organize a Hematopoietic Microenvironment." Cell **131**(2): 324-336.

Shabani, I., V. Haddadi-Asl, M. Soleimani, E. Seyedjafari and S. M. Hashemi (2014). "Ion-Exchange Polymer Nanofibers for Enhanced Osteogenic Differentiation of Stem Cells and Ectopic Bone Formation." ACS Applied Materials & Interfaces **6**(1): 72-82.

Shanmugasundaram, N., P. Ravichandran, P. Neelakanta Reddy, N. Ramamurty, S. Pal and K. Panduranga Rao (2001). "Collagen–chitosan polymeric scaffolds for the in vitro culture of human epidermoid carcinoma cells." Biomaterials **22**(14): 1943-1951.

Simonsen, J. L., C. Rosada, N. Serakinci, J. Justesen, K. Stenderup, S. I. S. Rattan, T. G. Jensen and M. Kassem (2002). "Telomerase expression extends the proliferative life-span and maintains the osteogenic potential of human bone marrow stromal cells." Nat Biotech **20**(6): 592-596.

Thomas, L. V. and P. D. Nair (2011). "(Citric acid-co-polycaprolactone triol) polyester: a biodegradable elastomer for soft tissue engineering." Biomatter **1**(1): 81-90.

Tollemar, V., Z. J. Collier, M. K. Mohammed, M. J. Lee, G. A. Ameer and R. R. Reid (2016). "Stem cells, growth factors and scaffolds in craniofacial regenerative medicine." Genes & Diseases **3**(1): 56-71.

Tomlinson, M., C. Dennis, X. Yang and J. Kirkham (2015). "Tissue non-specific alkaline phosphatase production by human dental pulp stromal cells is enhanced by high density cell culture." Cell and Tissue Research: 1-12.

Wang, X., B. Ding and B. Li (2013). "Biomimetic electrospun nanofibrous structures for tissue engineering." Materials Today **16**(6): 229-241.

Wu, C., Y. Zhou, J. Chang and Y. Xiao (2013). "Delivery of dimethyloxallyl glycine in mesoporous bioactive glass scaffolds to improve angiogenesis and osteogenesis of human bone marrow stromal cells." Acta Biomaterialia **9**(11): 9159-9168.

Yang, F., J. Wang, J. Hou, H. Guo and C. Liu (2013). "Bone regeneration using cell-mediated responsive degradable PEG-based scaffolds incorporating with rhBMP-2." Biomaterials **34**(5): 1514-1528.

Zhu, Y., C. Gao, X. Liu and J. Shen (2002). "Surface modification of polycaprolactone membrane via aminolysis and biomacromolecule immobilization for promoting cytocompatibility of human endothelial cells." Biomacromolecules **3**(6): 1312-1319.

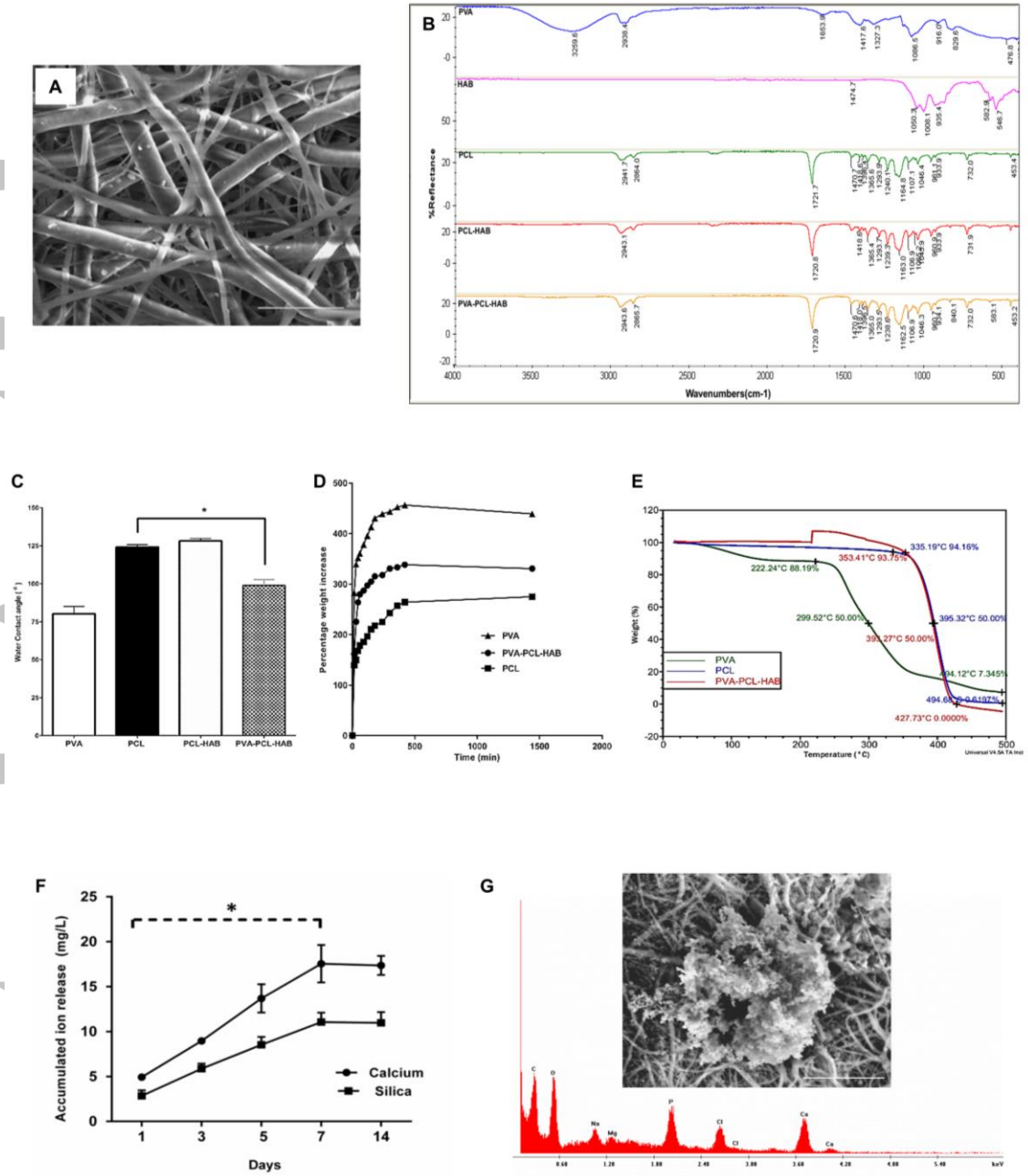

Fig.1. Physicochemical characterization.

(A) Scanning Electron Microscopic (SEM) image PVA-PCL-HAB (Scale bar: 5 µm). (B) Stacked FTIR spectra shows peaks of PVA, HAB, PCL, PCL-HAB and PVA-PCL-HAB. (C) Water Contact angle measurement of PVA, PCL, PCL-HAB and PVA-PCL-HAB. (* P< 0.05) (D) Swelling profile of PCL, PVA-PCL-HAB and PCL (E) Thermogram of PVA, PCL and PVA-PCL-HAB. (F) ICP-OES analyses of ion washout PVA-PCL-HAB. (* P< 0.05) (G) SEM (Scale bar: 50 µm) and Electron Dispersive X-ray spectra shows apatite crystals formation at day 30 after immersion in Stimulated Body Fluid.

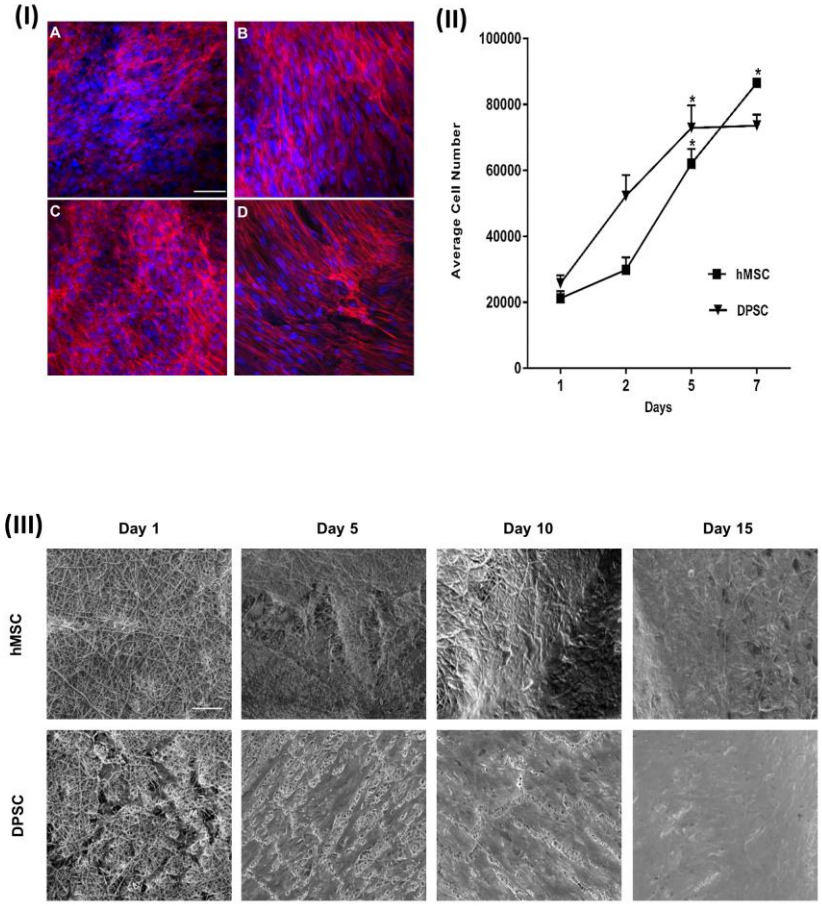

Fig.2. Cell attachment, proliferation and spreading

(I) Dapi / Phalloidin staining. Confocal microscopy of Dapi / Phalloidin stained cells attached on PVA-PCL-HAB (Scale bar: 100 µm) (A) hMSC day 1 (B) hMSC day 7 (C) DPSC day 1 (D) DPSC day 7 **.**

(II) Cell proliferation assay. A significant increase (* $P< 0.05$) in cell number was detected for both hMSC and DPSC on PVA-PCL-HAB.

(III) Cell proliferation and spreading on PVA-PCL-HAB. Scanning Electron Microscopy (Scale bar: 50µm).

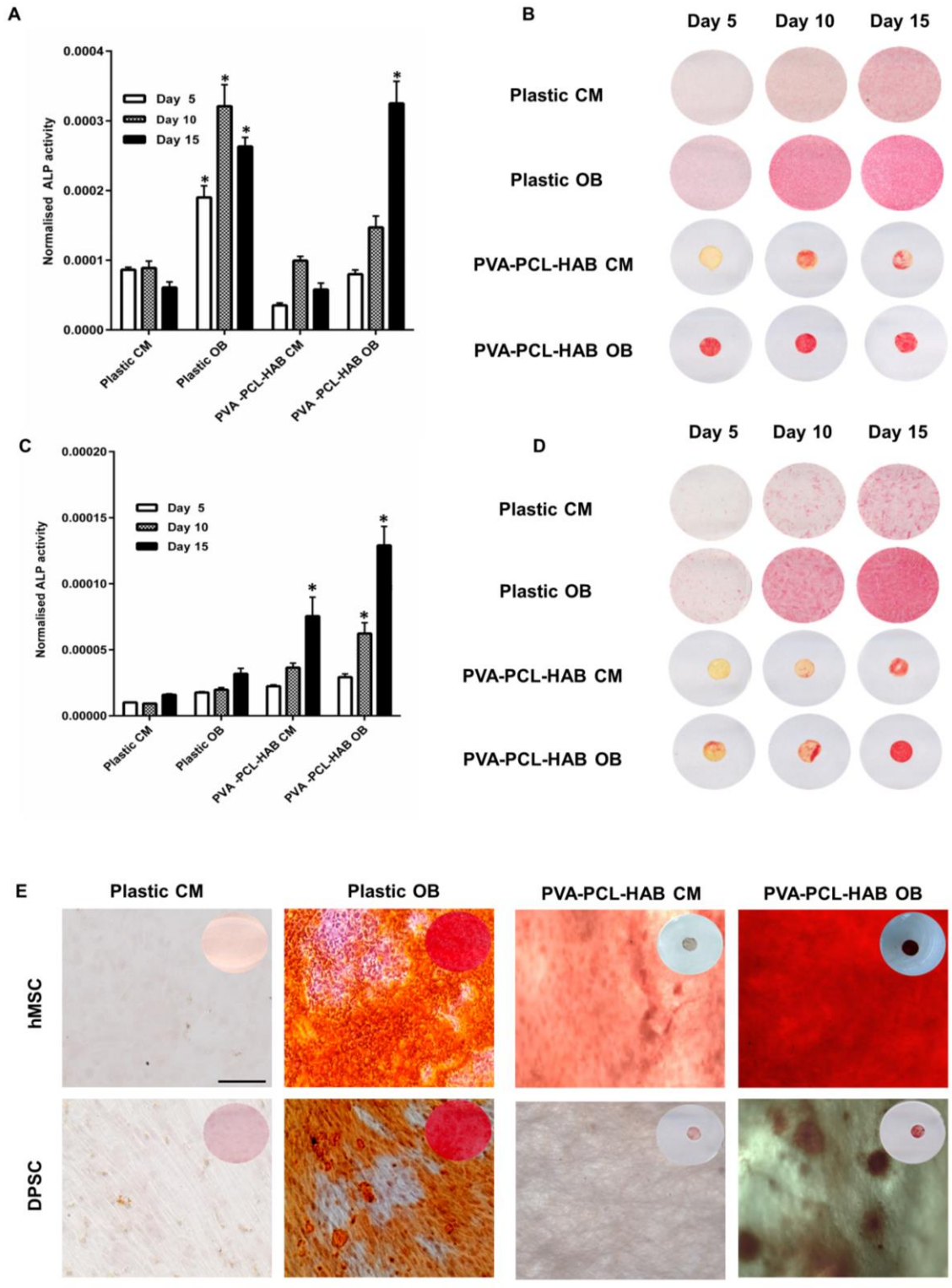

Fig.3. Osteoblastic differentiation and mineralization.

(A) ALP activity hMSC (*P<0.05) (B) ALP staining hMSC (C) ALP activity DPSC (*P<0.05) (D) ALP staining DPSC (E) Alizarin RED staining (Scale bar : 200 µm) ; inset shows macroscopic view

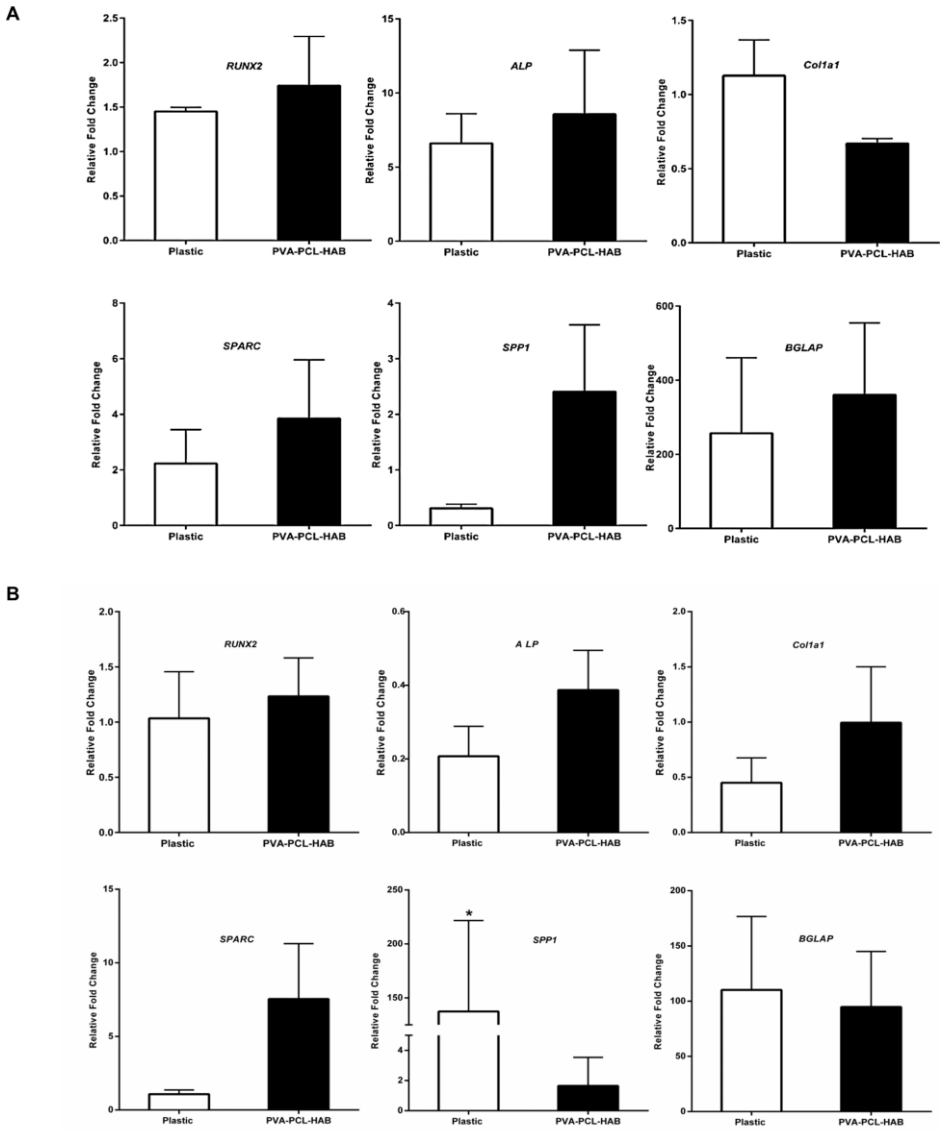

Fig.4. Osteogenic gene expression

Relative fold change by RT-qPCR analysis at day 15 on Plastic and PVA-PCL-HAB (*P<0.05)

(A) hMSC (B) DPSC

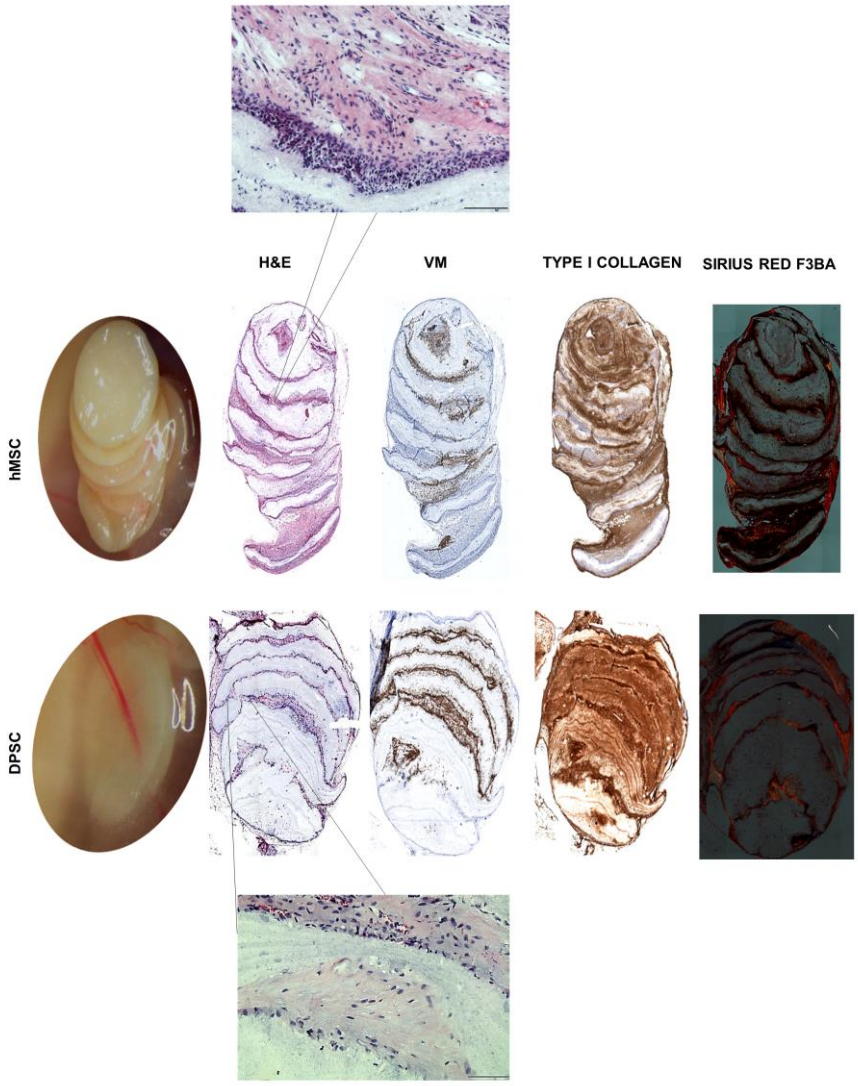

Fig. 5. *In vivo* implantations in NOD-SCID mice.

At eight weeks, ectopic bone formation on subcutaneous implantation demonstrate blood vessel ingrowth seen both cell groups (hMSC and DPSC). Histology mosaic image (10x) magnification and the inset (H&E) shows bone formation and cell migration through PVA-PCL-HAB. Human Anti vimentin (VM) stain shows presence of cells of human origin